Talanta 81 (2010) 1197–1202

Contents lists available at ScienceDirect

Talanta

journal homepage: www.elsevier.com/locate/talanta

Amperometric glucose biosensor based on biocompatible poly(dimethylaminoethyl) methacrylate microparticles

J.P. Hervás Pérez [a], E. López-Cabarcos [b], B. López-Ruiz [a,*]

[a] Sección Departamental de Química Analítica, Facultad de Farmacia, Universidad Complutense de Madrid, Ciudad Universitaria s/n, 28040 Madrid, Spain
[b] Departamento de Físico-Química Farmacéutica, Facultad de Farmacia, Universidad Complutense de Madrid, 28040 Madrid, Spain

ARTICLE INFO

Article history:
Received 16 July 2009
Received in revised form 25 January 2010
Accepted 4 February 2010
Available online 11 February 2010

Keywords:
Amperometric biosensor
Dimethylaminoethyl methacrylate
Glucose oxidase
Microparticles

ABSTRACT

Glucose oxidase (GOx) has been immobilized within poly(dimethylamino) ethyl methacrylate (p-DMAEM) microparticles which were subsequently used as biological material in the fabrication of a glucose biosensor. The enzyme immobilization method was optimized in relation with the monomer concentration and cross-linker content. It was found that the best biosensor response corresponds to microparticles synthesized with 1.19 M monomer and 0.37% cross-linking content. Furthermore, the influence on the biosensor response of parameters such as working potential, pH, temperature, and loaded enzyme were investigated. In addition, analytical properties such as sensitivity, linear range, response time, and detection limit were determined. The biosensor was used to analyze glucose in human serum samples with satisfactory results. The useful lifetime of the biosensor is at least 520 days.

1. Introduction

Research on glucose biosensors has attracted great interest due to the increasing incidence of diabetes in the population of developed countries and the need of such devices to monitor glucose levels [1,2]. The fabrication of biosensors with biocompatible materials will allow the monitorization *in vivo* of glucose and other compounds. Future progress in biosensors design will certainly focus upon the technology of new materials that solve the biocompatibility problem. Another decisive factor is the immobilization of enzymes, with complete retention of their biological activity, in matrices with good diffusion properties for substrates. Various methods for enzyme immobilization have been assayed such as covalent binding [4,5], entrapment in a suitable matrix [6,7], adsorption onto insoluble materials [8], conjugation [9], ionic-covalent hybridation [10,11], etc. Materials with hydrogel-like properties are good candidates to solve the above problems since they are generally biocompatible due to their high water content [3], can be used to immobilize enzymes, and their porosity can be varied controlling the cross-linker content during the synthesis.

After the pioneer work of Wichterle and Lim in the sixties [18], the use of methacrylate hydrogels in biomedical applications has made remarkable progresses in the field of biosensors, drug delivery systems, contact lenses, and synthetic membranes [7,11,19–23]. Among methacrylates p-DMAEM (see Scheme 1) is widely used as drug delivery system, and in contact lenses since is biocompatible, pH sensitive, and thermoresponsive [24–30].

In the present work, GOx from *Aspergillus niger* (EC 1.1.3.4) was taken as model redox enzyme because of its high stability, good catalytic ability, commercial availability, and moderate cost. Moreover, GOx is a widely studied enzyme that provides a suitable model system for the development of enzyme electrodes [12–17].

We have investigated GOx immobilization in p-DMAEM matrices with the aim to compare the results obtained with this biosensor and those previously reported by our group using different polymer immobilization system [31–33]. Biosensors prepared with p-DMAEM present an improvement in sensibility and maximum current density in comparison with previous reported devices.

2. Experimental

2.1. Chemicals

DMAEM, GOx (EC 1.1.3.4) (425 IU/mL) from *A. niger*, D+glucose, ascorbic acid, uric acid and Nafion 5 wt.% (Nafion purum 5% in a mixture of lower aliphatic alcohols and water), were purchased from Sigma (St. Louis, MO, USA). *N*,*N*′-methylenebisacrylamide (BIS) from Aldrich (St. Louis; MO, USA), ammonium persulfate, *N*,*N*,*N*′,*N*′-tetramethylethylendiamine (TEMED) and the surfactant Span 80 from Fluka (Buchs, Switzerland). Acetate/phosphate buffer solutions were prepared from stock solutions of sodium dihydrogen phosphate and sodium acetate (Panreac). The dialysis membrane (12,000–14,000 MWCO) was purchased from Spectrum Medical

* Corresponding author. Tel.: +34 91 394 1756; fax: +34 91 394 1754.
E-mail address: bealopru@farm.ucm.es (B. López-Ruiz).

0039-9140/$ – see front matter © 2010 Elsevier B.V. All rights reserved.
doi:10.1016/j.talanta.2010.02.010

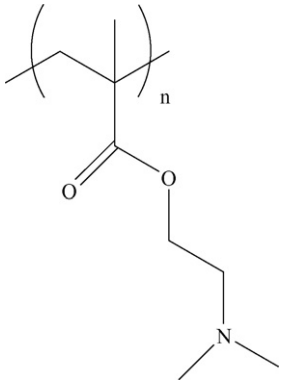

Scheme 1. Structure of p-DMAEM.

Industries. All reagents were used as received and the water was Milli Q quality (Millipore, Milford, MA, USA).

2.2. Apparatus and measurements

Scanning electron micrographs (SEM) of the microparticles were obtained with a JEOL JSM-6400 microscope operating at an acceleration voltage of 20 kV and 5000× magnification. The grid with the microparticles was dried, and replicas were produced by shadowing with gold deposited with a Balzers Sputter Coater (SCD-004). Particle size measurements in the range 2–150 μm were performed with a Galai-Cis-1 particle analyzer system. The pH of the buffer solution was adjusted using a Metler Toledo MP-230 pH-meter. Amperometric measurements at constant potential were carried out at a Metrohm Polarecord Potentiostat, Model E-506. Electrochemical measurements were performed in 0.05 M acetate/0.05 M phosphate buffer and in 0.1 M phosphate buffer, using a three-electrode cell with a platinum electrode as working electrode, a SCE reference electrode and a platinum counter electrode. Calibration plots were obtained by measuring the current response, after successive additions of substrate solution into a stirred electrolyte solution (10 mL), corresponding to the enzyme saturation concentration. The linear part of these calibration plots was fitted in order to obtain the best correlation coefficient R^2. Sensitivity was expressed as the slope of the calibration curve. Detection limit was calculated according with the criterion of ratio signal-to-noise equal 3. The response time was the time needed to reach 95% of the steady-state current after a substrate addition.

2.3. Emulsion preparation and microparticles synthesis

p-DMAEM microparticles with varying amount of BIS were prepared using the concentrated emulsion polymerization method, following the procedure previously published [34]. The immobilization of GOx was carried out by adding the enzyme (425 IU mL^{-1}) to the aqueous phase of the concentrated emulsion. The amount of cross-linking ($\eta = n_{BIS}/(n_{BIS} + n_{monomer})$% where n_{BIS} and $n_{monomer}$ are the number of moles of BIS and monomer respectively) was varied between 0.25% and 1.48%. During the synthesis of the microgels (around 1.5 h) the temperature was controlled and kept below 25 °C to preserve the enzyme properties.

2.4. Overall reaction of the glucose biosensor

The electrode surface (diameter 3 mm) was polished with 0.05 μm alumina slurry paste. After polishing, any residual abrasive particles were removed ultrasonically in ethanol and subsequently in distilled water. An exactly weighed amount of microgel particles was placed on the electrode surface and fixed with a dialysis membrane. The resulting electrode was washed with phosphate buffer and overoxidized at +0.6 V vs. SCE until the background current decreased to a constant level.

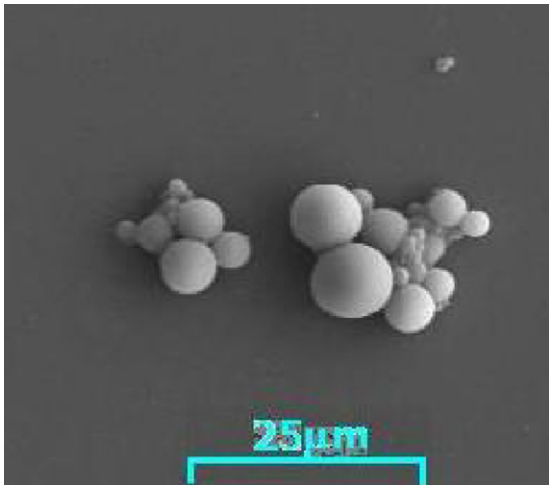

Fig. 1. SEM micrograph of freeze-dried p-DMAEM microparticles with entrapped GOx.

The biosensor response is based on an indirect measurement that correlates the amount of glucose with the concentration of hydrogen peroxide. Because the redox centres in GOx are buried within the molecule, direct electron transport to the surface of the electrode does not occur to any measurable degree. GOx is first reduced by the substrate glucose and then reoxidized by oxygen. Oxygen behaves as electron acceptor for reduced GOx leading to the formation of hydrogen peroxide that is oxidized at the electrode and the resulted current is detected by amperometry.

3. Results and discussion

3.1. Characterization of the microparticles

Fig. 1 illustrates a micrograph of p-DMAEM microparticles with entrapped GOx prepared with $\eta = 0.37$%, the microgels are spherical and polydisperse.

As Fig. 2 shows, the concentrated emulsion polymerization method produces microparticles with entrapped GOx whose diameters lie between 2 and 12 μm. The average size was 4.94 μm very

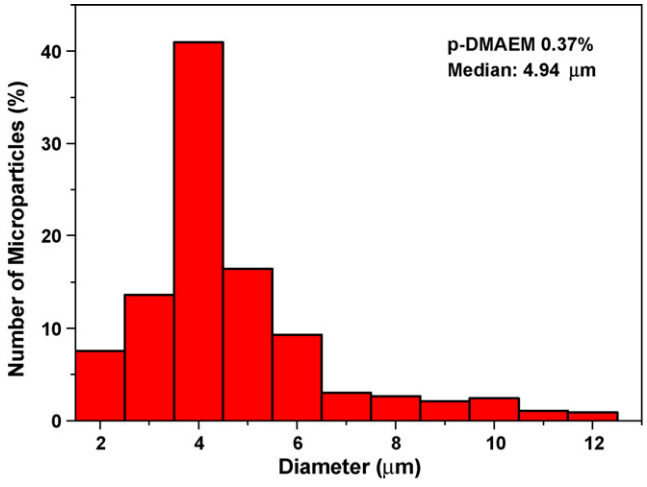

Fig. 2. Size distribution of the p-DMAEM microparticles with entrapped GOx, in phosphate buffer pH 6.0 and 25 °C.

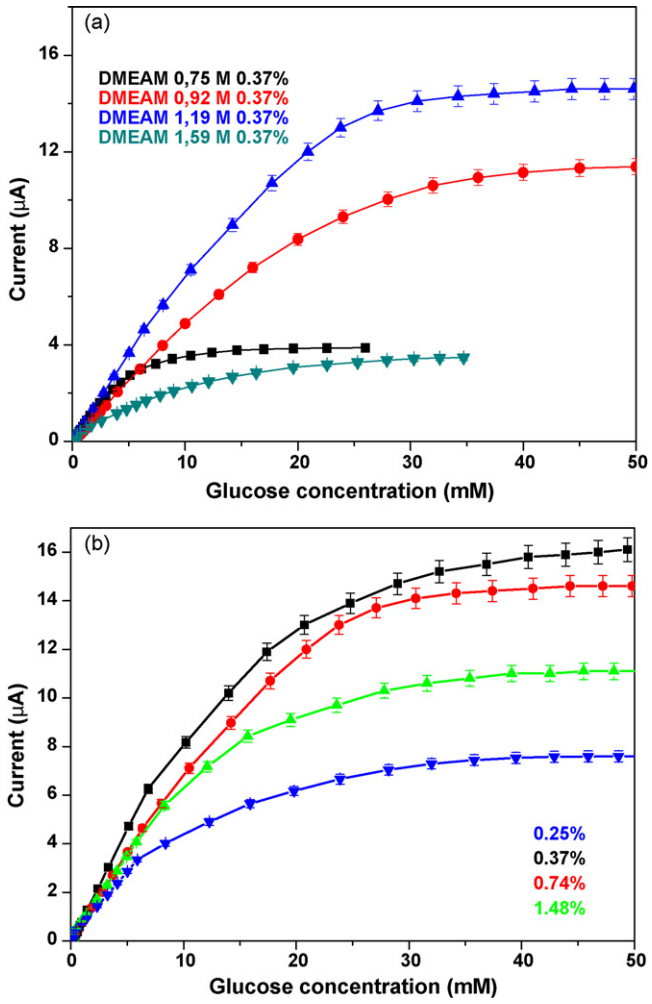

Fig. 3. Calibration curves for glucose, as a function of monomer concentration of the microgel (cross-linking 0.37%) (a) and cross-linking content (1.19 M of monomer) (b), in a stirred 0.1 M phosphate buffer solution, pH 6.0, potential of +0.6 V vs. SCE and 25 °C.

close to the 5 μm average size of the microparticles prepared without GOx and with the same cross-linking content. As can be seen in Fig. 2, around 75% of the microparticles present a size comprised between 3 and 5 μm.

3.2. Optimization of the synthesis method

3.2.1. Monomer concentration

Fig. 3a shows the steady-state response curves obtained at the platinum electrode with p-DMAEM microparticles synthesized at pH 6.0, $\eta = 0.37\%$, containing 425 IU mL^{-1} of GOx, and different concentration of monomer in the aqueous phase (0.75, 0.92, 1.19, and 1.59 M). The maximum current response was found for monomer concentration 1.19 M. A further increase in the monomer concentration decreases the current response. This behaviour is attributed to the decreasing of pore size with increasing monomer concentration that introduces a higher diffusional barrier hindering the motion of both, the substrate towards the enzyme catalytic site, and the product of the enzymatic reaction towards the electrode. Decreasing the monomer concentration down to 0.75 M also results in a decrease of the response due to the loss of immobilized enzyme as it was demonstrated by measuring enzymatic activity in the supernatant liquid obtained after the synthesis of the microgels.

Table 1
Kinetics of degradation of enzyme entrapped in microparticles with 0.37%. Experimental conditions: 0.1 M phosphate buffer pH 6.0 and +0.6 V vs. SCE.

Temperature (°C)	Current $t = 0$ s (nA)	Current $t = 60$ s (nA)	Percentage of degradation
25	350	350	0.0
30	445	445	0.0
35	475	435	8.4
40	495	445	10.1

3.2.2. Effect of the cross-linking content

Microparticles with different amount of cross-linking, η, were prepared with the aim to optimize the pore size of the polymer matrix for preparation of biosensors. Fig. 3b shows the calibration curves of the biosensor response vs. glucose concentration for microparticles with cross-linking between 0.25% and 1.49%. The monomer concentration selected to obtain these curves was 1.19 M, and the amount of entrapped GOx was 425 IU/mL.

The optimum response occurs for microgels with $\eta = 0.37\%$. Microparticles prepared with lower fractions of cross-linking present a pore size too large to efficiently retain the enzyme. By contrast, the decrease of the response for $\eta \geq 0.37\%$ is attributed to a higher substrate diffusional barrier imposed by the cross-linking. Accordingly, microparticles with $\eta = 0.37\%$ and monomer concentration 1.19 M were selected for subsequent measurements performed in this work to optimize the biosensor response with respect to the working conditions.

3.3. Optimization of the biosensor response

3.3.1. Working potential

The dependency of the biosensor response (steady-state current at the electrode) on the applied potential was investigated in 0.1 M phosphate buffer solution, pH 6.0, containing 0.25 mM glucose. The response of the enzyme electrode increased with the applied potential up to +0.60 V vs. SCE and levels off for higher values. The operating potential of +0.60 V vs. SCE was used in all subsequent measurements.

3.3.2. Temperature

The effect of the temperature on the biosensor response at 30 mM glucose was studied in the interval 0–60 °C performing all measurements under oxygen saturation conditions and keeping the pH constant at 6.0. As can be seen in Fig. 4a, the optimum temperature lies between 35 and 45 °C. The temperature of maximum activity of the free enzyme was 30 °C [35]. It seems that the immobilizing matrix slightly improves the thermal stability of the enzyme. In order to check the enzyme stability in this temperature range we have investigated the kinetics of degradation keeping constant the temperature for 1 h and measuring the current intensity on time 0 and after 60 min, The results presented in Table 1 indicate that when the temperature surpasses 30 °C the current decreases due to the beginning of enzyme denaturation.

However, the loss of the activity of the immobilized enzyme is slower than that of the free enzyme, and it seems that the polymer matrix has a somewhat protective effect at high temperatures. It has been reported, that the conformational flexibility of enzymes is affected by immobilization which is reflected by an increase in the stability towards denaturation by raising the temperature [36,37]. According to the above results, 30 °C was chosen as working temperature for all further experiments.

As is shown in Fig. 4b, the Arrhenius plot presents two regions. The activation energies calculated from the slopes and were 23.31 and 43.11 kJ/mol. The activation energy in the low temperature region is significantly higher than the one reported for the free enzyme, 14.6 kJ/mol [38]. Similar activation energies of 26.60 and

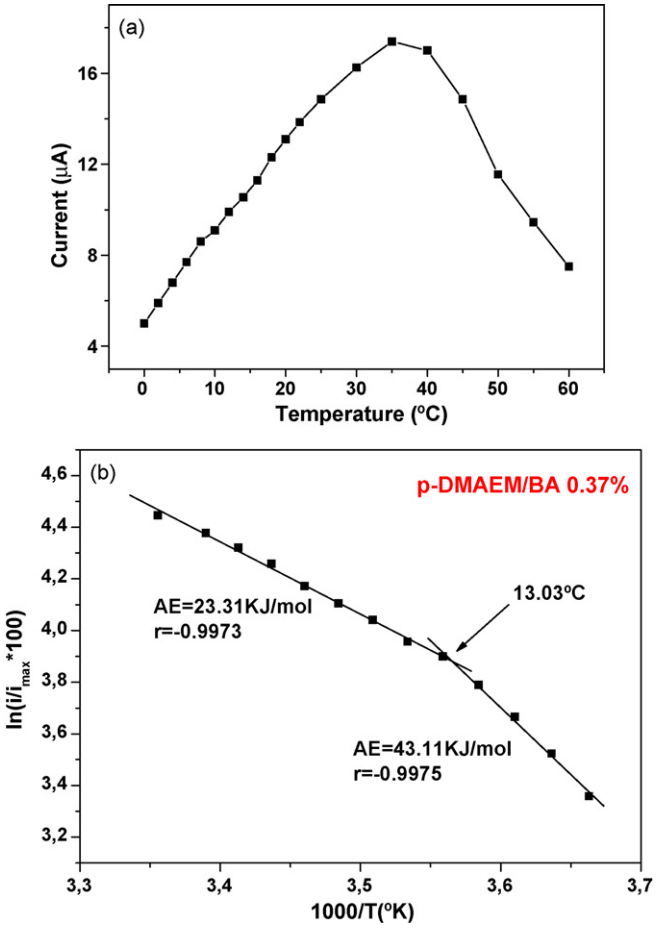

Fig. 4. Effect of working temperature on the biosensor response (a), and Arrhenius plot (b) for GOx immobilized in p-DMAEM, $\eta = 0.37\%$, 30 mM of glucose. Experimental conditions as in Fig. 3.

50.46 kJ/mol were reported for GOx immobilized in polyacrylamide microgels [31], and of 15.43 and 48.58 kJ/mol for GOx immobilized in poly(ethylene glyol) methyl ether methacrylate microparticles [32]. It seems that GOx has a disfavourable conformation in the immobilized state, resulting in a smaller catalytic effect compared to the free enzyme.

Thermoresponsive polymers exhibit a conspicuous volume phase transition from swollen to collapsed states which could also influence the enzymatic activity [31,33,39,40]. Thus, the two linear regions observed in the Arrhenius plots would roughly be associated with the two different polymer environments surrounding the entrapped enzyme [38,41]. The transition from de swollen to the collapse states of the microgel might provoke changes not only in enzyme conformation but also in enzyme accessibility for the substrate.

3.3.3. pH

The influence of pH on the glucose biosensor response to 30 mM glucose was checked in 0.05 M acetate/0.05 M phosphate buffer solutions from pH 4.0 to 8.0 at 25 °C. The optimal pH was found to be 6.0 coincident with the optimum pH reported for the free enzyme which indicates the catalytic function of GOx is not affected by the immobilization process.

3.3.4. Loading

Glucose levels of diabetic patients are higher than 5 mM, therefore, with the aim of a possible application, we have extended the calibration range of the biosensor. Based on previous works [32] we have chosen as reference an enzymatic load of 765 IU/mL and we tested two methods of modifying the amount of enzyme in the surface of the electrode: (i) changing the amount of enzyme immobilized within the microgel, and (ii) varying the amount of microparticles placed on electrode surface. The linear range reaches 8.0×10^{-3} and 6.0×10^{-3} M when the amount of GOx used in the synthesis is 255 and 765 IU/mL respectively. These values slightly increased by increasing the amount of microparticles placed on the electrode surface from 1 up to 3 mg. However in both cases the sensitivity increased and for this reason we have selected for later experiments microparticles prepared with 765 IU/mL GOx and a load of 3 mg of microparticles on the electrode. Table 2 summarizes the analytical properties of the biosensors prepared with the later conditions.

3.4. Analytical properties

Under optimal conditions ($\eta = 0.37\%$, potential +0.6 V, pH 6.0 and 30 °C), we realized a calibration curve in which the glucose biosensor presented the following properties: sensitivity of 23.4 mA M^{-1} cm^{-2}, maximum current density 264.7 μA cm^{-2}, linear range between 9.0×10^{-6} and 6.0×10^{-3} M, and detection limit 1 μM. These results present an improvement in sensitivity (from 17.8 up to 23.4 mA M^{-1} cm^{-2}) and maximum current density (from 114.3 to 264.7 μA cm^{-2}) when compared with similar immobilization systems (polymeric microparticles) previously reported [31–33].

The precision of the biosensor was evaluated in terms of repeatability by performing 10 successive measurements at different substrate solutions. The glucose concentration of the solutions covered the whole linear range (0.25, 2.5, and 5.0 mM). The relative standard deviation (RSD) obtained for each concentration was 5.7%, 2.9%, and 1.8% respectively. Our results were compared with those obtained using the Horwitz equation [42], RSD (%) = $2^{(1-0.5 \log C)}$, and in all cases the RSD was lower than the Horwitz accepted values. In addition, 20 measurements at 2.5 mM glucose (intermediate con-

Table 2
Analytical properties of the p-DMAEM biosensors as a function of the quantity of microparticles placed on electrode surface and the enzyme immobilized into the microparticles. Experimental conditions: 0.1 M phosphate buffer, pH 6.0 and +0.6 V vs. SCE.

Enzyme load		Sensitivity (mA M^{-1} cm^{-2})	J_{max} (μA cm^{-2})	Lineal range (M)	R^2 (N)[a]	DL (μM)
Quantity of microparticles in the biosensors (mg)	Quantity of enzyme in the microparticles (IU/mL)					
1	765	5.6	85.8	2.0×10^{-6} to 6.7×10^{-3}	0.9992 (18)	20
2	765	7.5	136.4	3.0×10^{-6} to 6.8×10^{-3}	0.9994 (18)	10
3	255	9.5	152.9	1.0×10^{-6} to 12.1×10^{-3}	0.9946 (22)	20
3	425	13.4	230.0	9.0×10^{-6} to 6.9×10^{-3}	0.9993 (21)	20
3	765	23.4	264.7	9.0×10^{-6} to 10.2×10^{-3}	0.9949 (26)	10
3	1020	10.2	192.3	8.0×10^{-6} to 6.0×10^{-3}	0.9992 (19)	10

[a] Points of linear range in calibration curve.

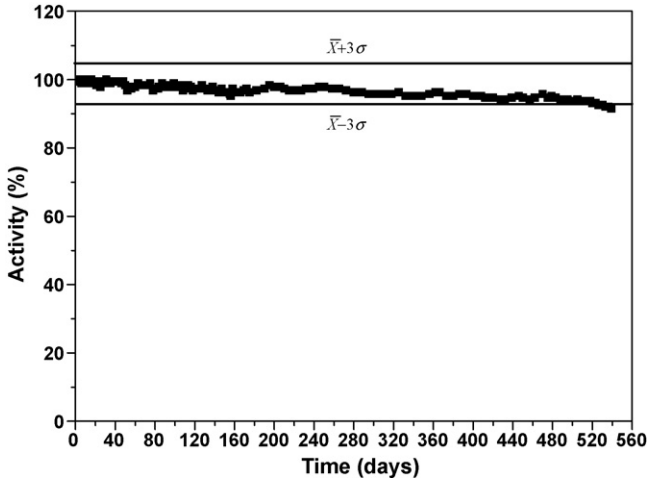

Fig. 5. Storage stability profiles for p-DMAEM biosensor. The biosensor was stored frozen in phosphate buffer at −4 °C when not in use.

centration) were performed at two different days. No changes were observed in the average value or in the data dispersion. When comparing the *p*-value corresponding to the averages and the variances of the measurements carried out each day (*p*-value = 0.8798 for averages and *p*-value = 0.8867 for variances) no statistically significant differences were observed.

The electrode stability was investigated during one and a half year (see Fig. 5). The electrode was stored in a frozen phosphate buffer solution pH 6.0 and periodically the response of the biosensor to 0.25 mM glucose solution was measured at potential +0.6 V vs. SCE, and at 30 °C. We have found that the biosensor exhibits an 85% of the initial signal 520 days after its preparation.

This biosensor improves significantly the stability, detection limit, and lineal range when compared with other devices prepared using different immobilization techniques such as layer-by-layer self-assembly films, or deposition on the electrode surface [43–46]. Thus, the detection limit is 10 times smaller than reported values, the linear range increases one order of magnitude, and the stability improves from 150 up to 520 days observed with this biosensor.

3.5. Interference study

The enzymatic electrode operates at a reading potential of +0.6 V vs. SCE corresponding to the oxidation of hydrogen peroxide. At this potential, the H_2O_2 detection is disturbed by the presence of interfering species such as uric acid (UA) and ascorbic acid (AA) when physiological samples are analyzed since these acids present negative charge at the working pH (6.0–7.0). The interferences caused by electroactive molecules were eliminated using a Nafion layer covering the electrode surface since Nafion is a negatively charged polyelectrolyte whose effect on the negatively charged substrates is noticeable.

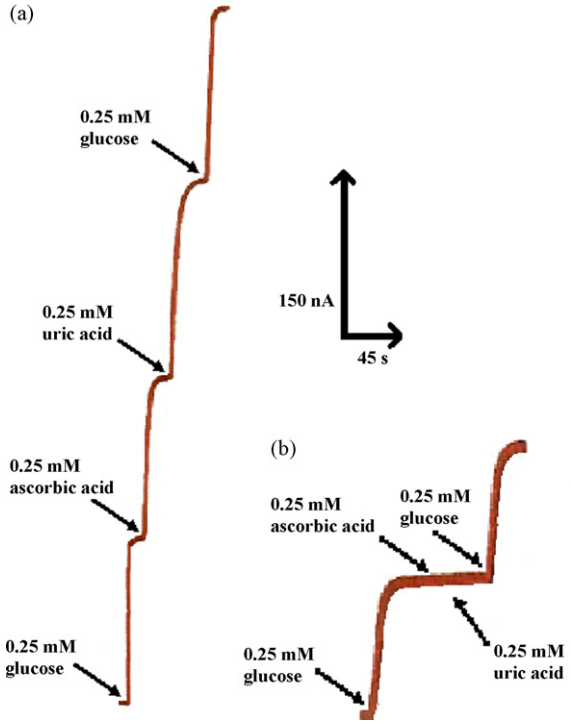

Fig. 6. GOx-biosensor response to 0.25 mM glucose, ascorbic and uric acids (a) and GOx-Nafion-biosensor response to 0.25 mM glucose, ascorbic and uric acids (b).

Thus, a layer of Nafion (50 μL) was applied on the electrode surface. The layer was dried in air for 15 min and subsequently the electrode was keeps at 80 °C for 45 min. The microparticles of p-DMAEM were then place over the Nafion film and covered with the dialysis membrane. As is shown in Fig. 6, for a biosensor prepared without Nafion (GOx-biosensor), the interfering signals of 0.25 mM uric acid and ascorbic acid are significant. On the contrary, when the GOx-Nafion-biosensor was calibrated, the signals arising from interferents disappeared (see Fig. 6). However, the current due to 0.25 mM of glucose was slightly affected and remains nearly constant, varying from 150 nA in the biosensor without Nafion to 145 nA in the biosensor with Nafion.

3.6. Human serum sample analysis

The glucose concentration of five serum pools were analyzed using both the GOx-biosensor and GOx-Nafion biosensor. The glucose of these serums was also analyzed by the spectrophotometric method of hexokinase [47] which was used as reference method. The result showed a good correlation with the reference method, especially in the case of the biosensor prepared with Nafion. The glucose concentration calculated with the biosensor without Nafion was always slightly higher than those obtained with the reference method due to the contribution of the ascorbic and uric acids

Table 3
Quantitative results obtained from the analysis of the serum by the spectrophotometric method (reference), GOx-biosensor, and GOx-Nafion-biosensor.

Sample	Glucose (mg/dl) reference method	Glucose[a] (mg/dl) GOx-biosensor	RSD (%)	GOx-biosensor deviations[b] (%)	Glucose[a] (mg/dl) GOx-Nafion biosensor	RSD (%)	GOx-Nafion biosensor deviations[b] (%)
1	93.0	97.7 ± 0.3	0.3	+4.8	93.5 ± 0.4	0.4	+0.5
2	89.0	93.0 ± 2.0	2.0	+4.3	88.0 ± 2.0	2.2	−0.8
3	99.0	105.0 ± 2.0	1.9	+6.1	100.7 ± 0.5	0.5	+1.7
4	91.0	92.0 ± 1.0	1.2	+1.0	90.0 ± 1.0	1.0	−0.9
5	83.0	85.0 ± 1.0	1.0	+2.2	82.9 ± 0.3	0.3	−0.1

[a] Average of three measurements.
[b] Deviation: deviation between the reference method and the biosensor results.

Table 4
Recovery studies using both glucose biosensors[a].

Sample	Glucose added (mg/dl)	GOx-biosensor		GOx-Nafion-biosensor	
		Glucose found[a] (mg/dl)	Recovery (%)	Glucose found[a] (mg/dl)	Recovery (%)
1	75.5	75.6 ± 0.9	100.2	76.0 ± 2	101.2
2	75.5	75.5 ± 0.9	100.1	76.0 ± 2	101.5
3	75.5	73.6 ± 0.9	97.5	76.0 ± 2	100.0
4	75.5	71.5 ± 0.9	94.8	75.0 ± 2	99.6
5	75.5	74.9 ± 0.9	99.3	76.0 ± 1	100.0

[a] Average of tree measurements

oxidation. By contrast, when Nafion was included in the biosensor, the concentration of glucose measured with both methods was similar and the values were never higher than 1.7% with positive and negative deviations. A good precision was obtained with the two biosensors RSD < 2.2% (Table 3). Furthermore, the recoveries observed with both biosensors were always between 94.8% and 101.5% (Table 4).

4. Conclusions

Microparticles based on p-DMAEM present an interesting matrix for GOx immobilization and can be used as biological element in glucose biosensors. The optimal conditions of the synthesis were: monomer concentration 1.19 M and η = 0.37%. Furthermore, the response of the biosensor is optimal for the following working conditions: pH 6.0; temperature 30 °C; 3 mg of particles on the electrode; and an enzyme load of 765 IU/mL. The significantly increasing of the stability, detection limit and lineal range, seem the most interesting characteristics of the proposed biosensors, compared with the biosensor previously reported by our research group. The interferences caused by species with negative net charge were eliminated by a Nafion layer covering the electrode surface. The biosensor has been successfully applied to the determination of glucose in serum samples. The biosensor maintains 85% of the initial response 18 months after the first use.

Acknowledgements

The authors acknowledge financial support from of the Spanish Science and Innovation Ministry (grant MAT2006-13646-C03-01), from the BSCH-UCM program for "Consolidation of Research Groups" (Group 911033, grant GR58/08; and Group 950247, grant PR1/08.15922-A), and from the COST Action D43. We also thank M.E. Gil-Alegre (Department of Pharmacy and Pharmaceutical Technology) and A. Rodriguez (Electron Microscopy Centre) for technical and professional assistance.

References

[1] B.D. Malhotra, A. Chaubey, Sens. Actuators B 91 (2003) 117.
[2] S. Chinnayelka, M.J. McShane, Biomacromolecules 5 (2004) 1657.
[3] V. Kudela, Encyclopaedia of Polymer Science and Engineering, vol. 7, Wiley, New York, 1987, p. 783.
[4] L. Doretti, D. Ferrara, S. Lora, G. Palma, Biotechnol. Appl. Biochem. 29 (1999) 67.
[5] S.H. Kim, S. Kim, V.K. Yadavalli, M.V. Pishko, Anal. Chem. 77 (2005) 6828.
[6] S. Brahim, D. Narinesingh, A. Guiseppi-Elie, Anal. Chim. Acta 448 (2001) 27.
[7] S. Brahim, D. Narinesingh, A. Guiseppi-Elie, Biosens. Bioelectron. 17 (2002) 53.
[8] G. Bayramoğlu, E. Yalçin, M.Y. Arica, Process Biochem. 40 (2005) 3505.
[9] T. Konno, J. Watanabe, K. Ishihara, Biomacromolecules 5 (2004) 342.
[10] F.N. Kok, F. Bozuglu, V. Hasirci, Biosens. Bioelectron. 17 (2002) 531.
[11] F.N. Kok, V. Hasirci, Biosens. Bioelectron. 19 (2004) 661.
[12] M. Portaccio, M. El-Masry, N.R. Diano, A. De Maio, V. Grano, M. Lepore, P. Travascio, U. Bencivenga, N. Pagliuca, D.G. Mita, J. Mol. Catal. B: Enzymatic 18 (2002) 49.
[13] L. Cen, K.G. Neoh, E.T. Kang, Biosens. Bioelectron. 18 (2003) 363.
[14] X. Liu, K.G. Neoh, L. Cen, E.T. Kang, Biosens. Bioelectron. 19 (2004) 823.
[15] H. Suzuki, A. Kumagai, K. Ogawa, E. Kokufuta, Biomacromolecules 5 (2004) 486.
[16] L.S. Bean, L.Y. Heng, B.M. Yamin, M. Ahmad, Thin Solid Films 477 (2005) 104.
[17] L.S. Bean, L.Y. Heng, B.M. Yamin, M. Ahmad, Bioelectrochemistry 65 (2005) 157.
[18] O. Wichterle, D. Lim, Nature, St. Martin's Press Inc., New York, 1960, p. 117.
[19] Y. Yang, S. Mu, H. Chen, Synth. Metals 92 (1998) 173.
[20] P. Van der Wetering, E.E. Moret, N.M.E. Schuuemans-Nieuwenbrock, M.J. Van Steenbergen, W.E. Hennik, Bioconjug. Chem. 10 (1999) 589.
[21] A. Blandino, M. Macias, D. Cantero, Process Biochem. 36 (2001) 601.
[22] E.J. Calvo, R. Etchenique, L. Pietrasanta, A. Wolosiuk, C. Danilowicz, Anal. Chem. 73 (2001) 1161.
[23] C.A. Marquette, L.J. Blum, Sens. Actuators B 90 (2003) 112.
[24] H. Yu, L.H. Gan, X. Hu, S.S. Venkatraman, K.C. Tam, Y.Y. Gan, Macromolecules 38 (2005) 9889.
[25] G. Zheng, H.D.H. Stover, Macromolecules 36 (2003) 7439.
[26] J. Du, Y. Tang, A.L. Lewis, S.P. Armes, J. Am. Chem. Soc. 127 (2005) 17982.
[27] J.V.M. Weaver, S.P. Armes, V. Bütün, Chem. Commun. 18 (2002) 2122.
[28] M. Sen, M. Sari, Eur. Polym. J. 41 (2005) 1304.
[29] Y.F. Chen, M. Yi, Acta Polym. Sin. 2 (2001) 215.
[30] K. Sutani, I. Kaetsu, K. Uchida, Radiat. Phys. Chem. 64 (2002) 331.
[31] B.J. Rubio Retama, E.J. López-Cabarcos, B. López-Ruiz, Talanta 68 (2005) 99.
[32] J.P. Hervás Pérez, E.J. López-Cabarcos, B. López-Ruiz, Talanta 75 (2008) 1151.
[33] M. Sánchez-Paniagua López, D. Mecerreyes, E. López-Cabarcos, B. López-Ruiz, Biosens. Bioelectron. 21 (2006) 2320.
[34] B.J. Rubio Retama, B. López-Ruiz, E.J. López-Cabarcos, Biomaterials 24 (2003) 2965.
[35] L. Ying, E.T. Kang, K.G. Neoh, J. Membr. Sci. 208 (2002) 361.
[36] M.A. Abdel-Naby, Appl. Biochem. Biotechnol. 38 (1993) 69.
[37] S.A. Cetinus, H.N. Oztop, Enzyme Microb. Technol. 32 (2003) 889.
[38] S. Cosnier, S. Szunerits, R.S. Marks, A. Novoa, L. Puech, E. Perez, I. Rico-Lattes, Talanta 55 (2001) 889.
[39] J.P. Hervás Pérez, M. Sánchez-Paniagua López, E. López-Cabarcos, B. López-Ruiz, Biosens. Bioelectron. 22 (2006) 429.
[40] M. Sánchez-Paniagua López, J.P. Hervás Pérez, E. López-Cabarcos, B. López-Ruiz, Electroanalysis 19 (2007) 370.
[41] D. Shan, M. Zhu, H. Xue, S. Cosnier, Biosens. Bioelectron. 22 (2007) 1612.
[42] W. Horwitz, Anal. Chem. 54 (1982) 67.
[43] S.A. Miscordia, J. Desbrieres, G.D. Barrera, P. Labbé, G.A. Rivas, Anal. Chim. Acta 578 (2006) 137.
[44] X. Chu, D. Duan, G. Shen, R. Yu, Talanta 71 (2007) 2040.
[45] B.Y. Wu, S.H. Hou, F. Yin, Zi.X. Zhao, Y.Y. Wang, X.S. Wang, Q. Chen, Biosens. Bioelectron. 22 (2007) 2854.
[46] L. Wu, X. Zhang, H. Ju, Biosens. Bioelectron. 23 (2007) 479.
[47] D.S. Young, Effects of Drug on Clinical Laboratory Test, 3rd edition, AACC Press, Washington, 1990.